Leader–Follower Formation Control of USVs With Prescribed Performance and Collision Avoidance

Shude He, Min Wang, *Member, IEEE*, Shi-Lu Dai, *Member, IEEE*, and Fei Luo

***Abstract*—This paper addresses a decentralized leader–follower formation control problem for a group of fully actuated unmanned surface vehicles with prescribed performance and collision avoidance. The vehicles are subject to time-varying external disturbances, and the vehicle dynamics include both parametric uncertainties and uncertain nonlinear functions. The control objective is to make each vehicle follow its reference trajectory and avoid collision between each vehicle and its leader. We consider prescribed performance constraints, including transient and steady-state performance constraints, on formation tracking errors. In the kinematic design, we introduce the dynamic surface control technique to avoid the use of vehicle's acceleration. To compensate for the uncertainties and disturbances, we apply an adaptive control technique to estimate the uncertain parameters including the upper bounds of the disturbances and present neural network approximators to estimate uncertain nonlinear dynamics. Consequently, we design a decentralized adaptive formation controller that ensures uniformly ultimate boundedness of the closed-loop system with prescribed performance and avoids collision between each vehicle and its leader. Simulation results illustrate the effectiveness of the decentralized formation controller.**

***Index Terms*—Collision avoidance, formation control, prescribed performance, unmanned surface vehicles (USVs).**

I. Introduction

COOPERATIVE or coordinated control of multiple unmanned marine vehicles has received considerable attention in system and control engineering during the last two decades due to its important applications such as cooperative exploration of ocean resources, distributed environmental monitoring, surveillance of territorial waters, and coordinated rescue missions [1], [2]. The fundamental idea of multiple-vehicle coordination is to use relatively inexpensive, simple, and small marine vehicles instead of an expensive specialized vehicle to cooperatively perform the complex tasks that usually cannot be accomplished by a single vehicle even with sophisticated equipment. One fundamental issue in multiple-vehicle coordination is formation control, whose objective is to achieve and maintain a predefined formation pattern such that the multiple vehicles could collaboratively accomplish a given task.

Several popular formation control design techniques including behavior-based control [3], virtual structures [4], and leader–follower architecture [5]–[7] have been proposed to fulfill the predefined formation shapes. Among these formation control design techniques, the leader–follower architecture is preferred in ocean engineering applications, e.g., to unmanned surface vehicles (USVs) [8]–[10], owing to its simplicity and scalability. The simplicity and scalability mainly stem from that the leader's motion related to the reference trajectory directs the group behavior and the follower could, in turn, serve as a leader for another vehicle, respectively. An efficient leader–follower formation control algorithm for a group of USVs was proposed in [8], where an approximation-based technique was employed to force vehicle formation moving along a desired trajectory with a given pattern. A distributed containment maneuvering controller for the USVs was proposed in [9], where each USV was subject to uncertain dynamics and unknown disturbances. An elegant leader–follower formation control scheme was presented for USVs [10], where the line-of-sight range and angle tracking errors were required to be constrained.

Although significant progress has been made in the leader–follower formation control of USVs, collision avoidances between the leaders and followers are not fully considered in the work mentioned above. Enforcing collision avoidance algorithms or the constraints of intervehicular distances in the formation control design is of great significance [11]. For a practical USV, the vehicle outputs, states, intervehicular distances, or tracking errors are often required to stay within the predefined constraint bounds due to system specifications or safety requirement. For example, the intervehicular distances among

Manuscript received August 31, 2017; revised February 10, 2018 and March 23, 2018; accepted April 24, 2018. Date of publication May 23, 2018; date of current version January 3, 2019. This work was supported in part by the National Natural Science Foundation of China under Grant 61773169, Grant 61473121, and Grant 61611130214, in part by the Guangdong Natural Science Foundation under Grant 2017A030313369 and Grant 2017A030313381, in part by the Science and Technology Planning Project of Guangdong Province under Grant 2017B010117007 and Grant 2017B090910011, and in part by the Fundamental Research Funds for the Central Universities. Paper no. TII-17-2026. *(Corresponding author: Min Wang.)*

The authors are with the School of Automation Science and Engineering, South China University of Technology, Guangzhou 510641, China (e-mail: shude_he@163.com; auwangmin@scut.edu.cn; audaisl@scut.edu.cn; aufeiluo@scut.edu.cn).

This paper has supplementary downloadable material available at http://ieeexplore.ieee.org.

Color versions of one or more of the figures in this paper are available online at http://ieeexplore.ieee.org.

Digital Object Identifier 10.1109/TII.2018.2839739

the USVs are required to preserve a certain distance to avoid collision when a group of USVs pass through the narrow waterways. Another important issue of formation control of USVs with modeling uncertainties concerns the transient performance of formation tracking errors. However, the analysis of transient and steady-state performance for the formation tracking errors has not been made systematically. Traditionally, formation tracking errors of approximation-based control systems could be verified to converge to a residual set [5]–[9], whose size depends on controller parameters and the upper bounds of approximation errors or/and external disturbances. However, there is still no available systematic procedure to precisely obtain the upper bounds. Furthermore, transient performance analysis for the closed-loop system is a challenging issue, especially when the vehicle dynamics are subject to modeling uncertainties [12]–[17] and unknown disturbances from maritime environments [18]–[20]. To guarantee the satisfaction of the prescribed transient and steady-state performances of output tracking errors, an elegant prescribed performance control (PPC) methodology was proposed in [21] for a nonlinear system. The PPC methodology was recently applied to design tracking controllers for nonlinear systems [22] and single mechanical systems, e.g., robot manipulators [23]–[25] and marine vehicles [26], where the prescribed performance controllers were designed in a centralized manner.

In this paper, we develop decentralized leader–follower formation control with prescribed performance and collision avoidance for a group of USVs with external disturbances. Both parametric uncertainties and uncertain nonlinear functions are discussed in the vehicle dynamics. To avoid potential collisions between neighboring vehicles, the position outputs of the USVs are constrained within a given range. To satisfy transient performance specifications, we enforce prescribed performance constraints on tracking errors in the formation control design. Based on the dynamic surface control (DSC) technique [27]–[29], the PPC methodology [21], adaptive control techniques [30]–[32], neural network (NN) approximators [33]–[37], the backstepping procedure, and the Lyapunov synthesis, we propose decentralized leader–follower formation control that guarantees the satisfaction of the prescribed performance constraints on formation tracking errors and the nonviolation of the collision avoidance constraint between the follower and its leader despite the presence of modeling uncertainties and external disturbances.

II. Problem Formulation and Preliminaries

A. USV Model

Consider a group of fully actuated USVs consisting of N USVs. The kinematics of the ith USV for $i \in \mathcal{N}$ with $\mathcal{N} = \{1, \ldots, N\}$ is described by

$$\dot{\boldsymbol{\eta}}_i = \mathbf{J}(\boldsymbol{\eta}_i)\boldsymbol{\nu}_i \tag{1}$$

where

$$\mathbf{J}(\boldsymbol{\eta}_i) = \begin{bmatrix} \cos\psi_i & -\sin\psi_i & 0 \\ \sin\psi_i & \cos\psi_i & 0 \\ 0 & 0 & 1 \end{bmatrix}$$

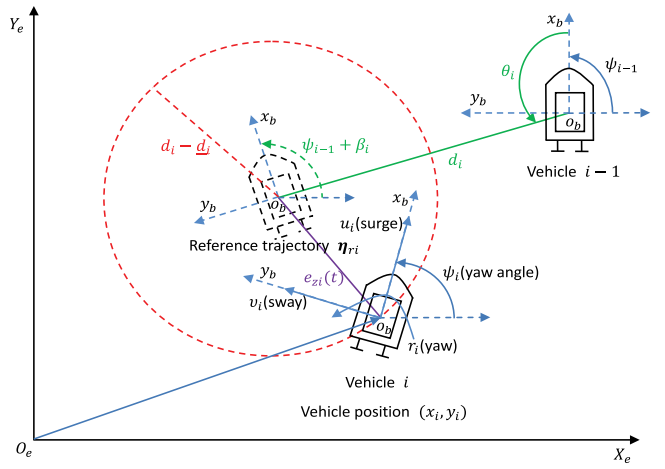

Fig. 1. Formation architecture of a pair of leader–follower. Each vehicle i ($i = 2, 3, ..., N$) should keep a suitable distance with respect to the reference trajectory $\boldsymbol{\eta}_{ri} = [x_{ri}, y_{ri}, \psi_{ri}]^T$ [defined in (4)]. To avoid collision between each vehicle i and its leader, the position errors $e_{zi}(t) < d_i - \underline{d}_i$, $i = 2, 3, ..., N$, should be satisfied for all $t \geq 0$, where $\underline{d}_i$ are the *safety* distances, which are predefined as the allowed minimal relative distances to avoid potential collision.

is the rotation matrix; $\boldsymbol{\eta}_i = [x_i, y_i, \psi_i]^T$ denotes the vehicle outputs, (x_i, y_i) is the position of the ith vehicle in the earth-fixed frame $O_eX_eY_e$, as shown in Fig. 1; ψ_i is the yaw angle; and $\boldsymbol{\nu}_i = [u_i, v_i, r_i]^T$ denotes the velocities, where u_i, v_i, and r_i are, respectively, the corresponding velocities in surge, sway, and yaw in the body-fixed frame $o_bx_by_b$ (see Fig. 1). Following the results in [38], the kinetics of the ith vehicle dynamics with modeling uncertainties and external disturbances can be written as

$$\mathbf{M}_i\dot{\boldsymbol{\nu}}_i = -\mathbf{C}(\boldsymbol{\nu}_i)\boldsymbol{\nu}_i - \mathbf{D}(\boldsymbol{\nu}_i)\boldsymbol{\nu}_i + \boldsymbol{\tau}_{wi}(t) + \boldsymbol{\tau}_i, \quad i \in \mathcal{N} \tag{2}$$

where $\mathbf{M}_i > 0$ is the inertia matrix, $\mathbf{C}(\boldsymbol{\nu}_i)$ is the total Coriolis and centripetal acceleration matrix, $\mathbf{D}(\boldsymbol{\nu}_i)$ is the uncertain hydrodynamic damping matrix, $\boldsymbol{\tau}_{wi} = [\tau_{w1i}, \tau_{w2i}, \tau_{w3i}]^T$ denotes the external disturbances, and $\boldsymbol{\tau}_i$ is the control inputs. The matrices $\mathbf{M}_i$, $\mathbf{C}(\boldsymbol{\nu}_i)$, and $\mathbf{D}(\boldsymbol{\nu}_i)$ are given by

$$\mathbf{M}_i = \begin{bmatrix} m_{11i} & 0 & 0 \\ 0 & m_{22i} & m_{23i} \\ 0 & m_{23i} & m_{33i} \end{bmatrix}$$

$$\mathbf{C}(\boldsymbol{\nu}_i) = \begin{bmatrix} 0 & 0 & c_{13i} \\ 0 & 0 & m_{11i}u_i \\ -c_{13i} & -m_{11i}u_i & 0 \end{bmatrix}$$

$$\mathbf{D}(\boldsymbol{\nu}_i) = \begin{bmatrix} d_{11i} & 0 & 0 \\ 0 & d_{22i} & d_{23i} \\ 0 & d_{32i} & d_{33i} \end{bmatrix} \tag{3}$$

with $c_{13i} = -m_{22i}v_i - m_{23i}r_i$, where $m_{11i} = m_i - X_{\dot{u}i}$, $m_{22i} = m_i - Y_{\dot{v}i}$, $m_{23i} = m_ix_{gi} - Y_{\dot{r}i}$, and $m_{33i} = I_{zi} - N_{\dot{r}i}$ are unknown parameters. Here, m_i is the mass of the ith vehicle; I_{zi} is the moment of inertia in yaw; $X_{\dot{u}i}$, $Y_{\dot{v}i}$, $Y_{\dot{r}i}$, and $N_{\dot{r}i}$ are the added masses; and x_{gi} is the x_b-coordination of the

ith vehicle center of gravity. The hydrodynamic damping terms d_{11i}, d_{22i}, d_{23i}, d_{32i}, and d_{33i} denote the modeling uncertainties because the damping terms are often difficult to obtain accurately [38], [39].

B. Leader–Follower Formation Architecture

Consider a decentralized leader–follower formation of N vehicles with a reference trajectory $\boldsymbol{\eta}_0 = [x_0, y_0, \psi_0]^T$. The reference trajectory $\boldsymbol{\eta}_0$ is designed according to the practical mission and is provided to the leading vehicle 1. Vehicle 1 serves as the global leader moving along the desired trajectory $\boldsymbol{\eta}_0$, and it does not follow any vehicle in the group. The vehicle i, $i = 2, 3, ..., N$, tracks its leader and maintains a prescribed formation pattern, while potential collision with its leader should be avoided. More specifically, there are many pairs of leader–follower, and the follower can, in turn, serve as the leader for another vehicle. As such, the formation with N vehicles could be decomposed into $N-1$ decentralized subsystems of two vehicles. The formation architecture of a pair of leader–follower is shown in Fig. 1, where the vehicle i ($i = 2, 3, ...N$) follows the vehicle $i-1$, and thus, the vehicle $i-1$ is the leader of vehicle i. A pair of leader–follower formation problem is described as follows: Given the leader's trajectory $\boldsymbol{\eta}_{i-1}$ (vehicle $i-1$), the reference trajectory $\boldsymbol{\eta}_{ri}$ to be tracked by the follower (vehicle i) is shifted by a desired distance d_i and angle θ_i and is rotated by an angle β_i relative to the leader (see Fig. 1), and then, the formation control objective is to design controller for vehicle i such that the vehicle i tracks its reference trajectory $\boldsymbol{\eta}_{ri}$ and avoids collision with its leader. Herewith, the reference trajectory $\boldsymbol{\eta}_{ri}$ to be tracked by vehicle i is given by

$$\boldsymbol{\eta}_{ri} = \boldsymbol{\eta}_{i-1} + \mathbf{J}(\boldsymbol{\eta}_{i-1})\boldsymbol{\eta}_{di}, \quad i \in \mathcal{N} \tag{4}$$

where $\boldsymbol{\eta}_{ri} = [x_{ri}, y_{ri}, \psi_{ri}]^T$, $\boldsymbol{\eta}_{i-1} = [x_{i-1}, y_{i-1}, \psi_{i-1}]^T$, $\boldsymbol{\eta}_{di} = [d_i \cos\theta_i, d_i \sin\theta_i, \beta_i]^T$, d_i ($d_1 = 0$, and $d_i > 0$, $i = 2, 3, ..., N$), β_i are the relative distance and heading angle between the reference trajectory $\boldsymbol{\eta}_{ri}$ and vehicle $i-1$, respectively, and θ_i is the desired angle between the reference position and the position of vehicle $i-1$. Herein, d_i, β_i, and θ_i are designer-specified parameters, and they could be either time-varying or time invariant. The time-varying parameters $d_i(t)$, $\beta_i(t)$, and $\theta_i(t)$ could be employed to reshape the formation pattern, which is competent to different missions. When $i = 1$, let $d_1 = 0$, $\beta_1 = 0$, and thus, we have $\boldsymbol{\eta}_{r1} = \boldsymbol{\eta}_0$ according to (4). When $i = 2, 3, ..., N$, d_i should be carefully specified to avoid the potential collision.

C. Collision Avoidance and Prescribed Performance

1) Collision Avoidance: Consider the collision avoidance between each vehicle and its leader in the leader–follower formation. Define the tracking errors between each vehicle i and the reference trajectory $\boldsymbol{\eta}_{ri}$ as follows:

$$\begin{aligned} e_{xi}(t) &= x_i(t) - x_{ri}(t) \\ e_{yi}(t) &= y_i(t) - y_{ri}(t) \\ e_{\psi i}(t) &= \psi_i(t) - \psi_{ri}(t). \end{aligned} \tag{5}$$

Then, the position tracking error is given by

$$e_{zi}(t) = \sqrt{e_{xi}(t)^2 + e_{yi}(t)^2}. \tag{6}$$

To avoid collision between the follower and its leader (see Fig. 1), the position error given in (6) is subject to the following condition:

$$e_{zi}(t) < d_i - \underline{d}_i \quad \forall t \geq 0;\ i = 2, 3, ..., N \tag{7}$$

where d_i is a desired distance defined in (4), and $\underline{d}_i$ ($\underline{d}_i > 0$, $i = 2, 3, ..., N$) denotes the *safety* distance, which means $\underline{d}_i$ is the allowed minimal relative distance to avoid potential collision.

2) Prescribed Performance Constraints: To satisfy transient performance specifications on the entire formation errors, we consider the following prescribed performance constraints:

$$-\underline{e}_{ji}(t) < e_{ji}(t) < \overline{e}_{ji}(t) \quad \forall t \geq 0;\ i \in \mathcal{N};\ j = x, y, \psi \tag{8}$$

with

$$\begin{aligned} \overline{e}_{ji}(t) &= (\overline{e}_{ji,0} - \overline{e}_{ji,\infty}) \exp(-\kappa_{ji} t) + \overline{e}_{ji,\infty} \\ \underline{e}_{ji}(t) &= (\underline{e}_{ji,0} - \underline{e}_{ji,\infty}) \exp(-\kappa_{ji} t) + \underline{e}_{ji,\infty} \end{aligned} \tag{9}$$

where $\overline{e}_{ji,0}$, $\overline{e}_{ji,\infty}$, κ_{ji}, $\underline{e}_{ji,0}$, and $\underline{e}_{ji,\infty}$ are positive designer-specified parameters, and $\overline{e}_{ji,\infty}$ and $\underline{e}_{ji,\infty}$ are the maximum allowable steady-state tracking errors with $\overline{e}_{ji,\infty} \leq \overline{e}_{ji,0}$ and $\underline{e}_{ji,\infty} \leq \underline{e}_{ji,0}$. Note that $\overline{e}_{ji}(t)$ and $\underline{e}_{ji}(t)$ are exponentially decaying functions, and thus, we could use inequality (8) and (9) to prescribe desired transient and steady-state performances of the formation errors.

Note that the bounds $-\underline{e}_{ji,0}$ and $\overline{e}_{ji,0}$ are designer-specified parameters, and we could appropriately choose them to satisfy the collision-free condition (7). The following corollary provides a sufficient condition for the collision avoidance between each vehicle and its leader.

Corollary 1: Consider tracking error constraint (8) with the boundary function (9). If the prescribed performance of tracking errors $e_{ji}(t)$ in the sense of (8) and (9) is guaranteed, and the maximum values of function (9) are chosen to satisfy

$$\sqrt{e_{mxi}^2 + e_{myi}^2} \leq d_i - \underline{d}_i, \quad i = 2, 3, ..., N \tag{10}$$

with $e_{mxi} = \max\{\overline{e}_{xi,0}, \underline{e}_{xi,0}\}$, $e_{myi} = \max\{\overline{e}_{yi,0}, \underline{e}_{yi,0}\}$, then each vehicle and its leader are *collision-free*, i.e., $e_{zi}(t) < d_i - \underline{d}_i$, $\forall t \geq 0$.

Proof: If the prescribed performance of tracking errors $e_{ji}(t)$ in the sense of (8) and (9) is guaranteed, then we have $|e_{ji}(t)| < \overline{e}_{ji}(t)$, or $|e_{ji}(t)| < \underline{e}_{ji}(t)$, $\forall t \geq 0$. Note that (9) is strictly decaying functions, and we have $\overline{e}_{ji}(t) \leq \overline{e}_{ji,0}$ and $\underline{e}_{ji}(t) \leq \underline{e}_{ji,0}$, $\forall t \geq 0$, which means $|e_{ji}(t)| < \max\{\overline{e}_{ji,0}, \underline{e}_{ji,0}\}$. Therefore, it follows from (6) and (10) that the inequality $e_{zi}(t) = \sqrt{e_{xi}(t)^2 + e_{yi}(t)^2} < \sqrt{e_{mxi}^2 + e_{myi}^2} \leq d_i - \underline{d}_i$ holds for all

$t \geq 0$, which means each vehicle and its leader are collision-free.

Assumption 1: The unknown time-varying external disturbance $\boldsymbol{\tau}_{wi}$ is bounded, i.e., $|\tau_{wli}| \leq \bar{\tau}_{wli}$, $l = 1, 2, 3$, with $\bar{\tau}_{wli}$ being unknown positive constants [40], [41].

Assumption 2: The reference trajectory $\boldsymbol{\eta}_0$ and its derivative $\dot{\boldsymbol{\eta}}_0$ are bounded. In the leader–follower formation architecture, the leading vehicle 1 tracks the reference trajectory $\boldsymbol{\eta}_0$, each vehicle i, $i = 2, 3, ..., N$, has a sole and fixed leader (vehicle $i-1$), and the vehicle i could obtain its leader's states $\boldsymbol{\eta}_{i-1}$ and $\boldsymbol{\nu}_{i-1}$ through their communication.

Assumption 3: At the initial time, the tracking errors satisfy $-\underline{e}_{ji}(0) < e_{ji}(0) < \overline{e}_{ji}(0)$, $i \in \mathcal{N}$.

Remark 1: If the design parameters d_i and θ_i in (4) satisfy $d_i = d_{i+1}$ and $\theta_i = \theta_{i+1}$ $(i = 2, ...N-1)$, and each USV satisfying Assumption 3 is positioned in a straight line at the initial time, then the collisions between neighboring vehicles could be avoided using Corollary 1.

Formation control objective: The objective of this paper is, under Assumptions 1–3, to design an adaptive control law $\boldsymbol{\tau}_i$ for each vehicle i $(i \in \mathcal{N})$ such that:

1) each vehicle i follows its reference trajectory $\boldsymbol{\eta}_{ri}$ given in (4);
2) the tracking errors $e_{ji}(t)$ in (5) remain within the predefined bounds $-\underline{e}_{ji}(t)$ and $\overline{e}_{ji}(t)$ defined in (9);
3) each vehicle i and its leader are *collision-free*, i.e., $e_{zi}(t) < d_i - \underline{d}_i$, $\forall t \geq 0$, $i = 2, 3, ...N$.

III. Adaptive Formation Control Design

Under the prescribed performance constraint (8) with (9) and (10), in this section, we design adaptive control for systems (1) and (2) to achieve the formation control objective.

A. Constrained Error Transformation

To design an adaptive controller that guarantees that constraint (8) with (9) and (10) is not violated, we introduce a smooth and strictly increasing error transformation function $T_{ji}(z_{ji})$ satisfying

$$\begin{cases} -\gamma_{ji} < T_{ji}(z_{ji}) < 1 \quad \forall z_{ji} \in \mathcal{L}_\infty \\ \lim\limits_{z_{ji} \to -\infty} T_{ji}(z_{ji}) = -\gamma_{ji} \\ \lim\limits_{z_{ji} \to +\infty} T_{ji}(z_{ji}) = 1 \\ T_{ji}(z_{ji}) = 0, \text{ iff } z_{ji} = 0 \end{cases} \tag{11}$$

with $\gamma_{ji}(t) = \underline{e}_{ji}(t)/\overline{e}_{ji}(t)$ for all $j = x, y, \psi$, $i \in \mathcal{N}$, where z_{ji} and $T_{ji}(z_{ji})$ are the *transformed error* and *transformation function* [21], respectively. In this paper, we could take $T_{ji}(z_{ji})$ as

$$T_{ji}(z_{ji}) = \frac{e^{z_{ji}} - e^{-z_{ji}}}{e^{z_{ji}} + \gamma_{ji}^{-1} e^{-z_{ji}}}. \tag{12}$$

To establish the relationship between e_{ji} and its boundary functions $\underline{e}_{ji}, \overline{e}_{ji}$, we define the following equation:

$$e_{ji} = \overline{e}_{ji} T_{ji}(z_{ji}). \tag{13}$$

Substituting (12) into (13), we obtain

$$e^{2z_{ji}} = \frac{\overline{e}_{ji} + e_{ji}\gamma_{ji}^{-1}}{\overline{e}_{ji} - e_{ji}}. \tag{14}$$

Taking the logarithm to both sides of (14) and noticing the equation $\gamma_{ji}(t) = \underline{e}_{ji}(t)/\overline{e}_{ji}(t)$, we obtain

$$z_{ji} = \frac{1}{2} \ln \left(\frac{\underline{e}_{ji} + e_{ji}}{\gamma_{ji}(\overline{e}_{ji} - e_{ji})} \right) \quad \forall j = x, y, \psi; \ i \in \mathcal{N} \tag{15}$$

where $\ln(\cdot)$ is the *natural logarithm*.

From (1), (5), and (15), the derivatives of z_{ji} are

$$\dot{z}_{xi} = p_{xi} \left(u_i \cos\psi_i - v_i \sin\psi_i - \dot{x}_{ri} \right) - q_{xi} \tag{16}$$

$$\dot{z}_{yi} = p_{yi} \left(u_i \sin\psi_i + v_i \cos\psi_i - \dot{y}_{ri} \right) - q_{yi} \tag{17}$$

$$\dot{z}_{\psi i} = p_{\psi i} (r_i - \dot{\psi}_{ri}) - q_{\psi i} \tag{18}$$

where

$$p_{ji} = \frac{1}{2} \left[\frac{1}{\underline{e}_{ji} + e_{ji}} + \frac{1}{\overline{e}_{ji} - e_{ji}} \right] \tag{19}$$

$$q_{ji} = -\frac{1}{2} \left[\frac{\dot{\underline{e}}_{ji}}{\underline{e}_{ji} + e_{ji}} - \frac{\dot{\overline{e}}_{ji}}{\overline{e}_{ji} - e_{ji}} - \frac{\dot{\gamma}_{ji}}{\gamma_{ji}} \right]. \tag{20}$$

Substituting (13) into (19) gives

$$p_{ji} = \frac{1}{2\overline{e}_{ji}} \left[\frac{1}{\gamma_{ji} + T_{ji}(z_{ji})} + \frac{1}{1 - T_{ji}(z_{ji})} \right]. \tag{21}$$

Using (21) and (11), we could obtain $p_{ji} > 0$.

B. Design of the Control Law

Step 1: Define the following coordinate transformation:

$$\mathbf{z}_{2i} = \boldsymbol{\nu}_i - \boldsymbol{\alpha}_{fi} \tag{22}$$

and the boundary layer error

$$\mathbf{e}_{\boldsymbol{\alpha}_i} = \boldsymbol{\alpha}_{fi} - \boldsymbol{\alpha}_i \tag{23}$$

where $\mathbf{z}_{2i} = [z_{21i}, z_{22i}, z_{23i}]^T$, and the filtered virtual control input vector $\boldsymbol{\alpha}_{fi} = [\alpha_{f1i}, \alpha_{f2i}, \alpha_{f3i}]^T$, the virtual control input vector $\boldsymbol{\alpha}_i = [\alpha_{1i}, \alpha_{2i}, \alpha_{3i}]^T$. Consider the following Lyapunov function candidate:

$$V_{0i} = \frac{1}{2} z_{xi}^2 + \frac{1}{2} z_{yi}^2 + \frac{1}{2} z_{\psi i}^2 \tag{24}$$

where z_{ji}, $j = x, y, \psi$, is defined in (15). Differentiating (24) along systems (16)–(18) gives

$$\begin{aligned} \dot{V}_{0i} = {} & z_{xi} \left[p_{xi} \left(u_i \cos\psi_i - v_i \sin\psi_i - \dot{x}_{ri} \right) - q_{xi} \right] \\ & + z_{yi} \left[p_{yi} \left(u_i \sin\psi_i + v_i \cos\psi_i - \dot{y}_{ri} \right) - q_{yi} \right] \\ & + z_{\psi i} \left[p_{\psi i} (r_i - \dot{\psi}_{ri}) - q_{\psi i} \right]. \end{aligned} \tag{25}$$

Consider equations (22), (23), and (25), and thus, the virtual control laws could be given by

$$\alpha_{1i} = \Phi_{1i}\cos\psi_i + \Phi_{2i}\sin\psi_i \tag{26}$$

$$\alpha_{2i} = -\Phi_{1i}\sin\psi_i + \Phi_{2i}\cos\psi_i \tag{27}$$

$$\alpha_{3i} = \frac{1}{p_{\psi i}}\left(-k_{z_{\psi i}} z_{\psi i} + q_{\psi i}\right) + \dot{\psi}_{ri} \tag{28}$$

where $\Phi_{1i} = \frac{1}{p_{xi}}(-k_{z_{xi}} z_{xi} + q_{xi}) + \dot{x}_{ri}$, $\Phi_{2i} = \frac{1}{p_{yi}}(-k_{z_{yi}} z_{yi} + q_{yi}) + \dot{y}_{ri}$, with control gains $k_{z_{xi}} > 0$, $k_{z_{yi}} > 0$, and $k_{z_{\psi i}} > 0$ being design parameters. Substituting the virtual control laws (26)–(28) into (25), we obtain

$$\dot{V}_{0i} = -k_{z_{xi}} z_{xi}^2 - k_{z_{yi}} z_{yi}^2 - k_{z_{\psi i}} z_{\psi i}^2 + \mathbf{z}_{2i}^T \mathbf{\Phi}_{3i} + \mathbf{e}_{\boldsymbol{\alpha}_i}^T \mathbf{\Phi}_{3i} \tag{29}$$

where $\mathbf{\Phi}_{3i} = [z_{xi} p_{xi}\cos\psi_i + z_{yi} p_{yi}\sin\psi_i, z_{yi} p_{yi}\cos\psi_i - z_{xi} p_{xi}\sin\psi_i, z_{\psi i} p_{\psi i}]^T$, and the coupling terms $\mathbf{z}_{2i}^T \mathbf{\Phi}_{3i}$ and $\mathbf{e}_{\boldsymbol{\alpha}_i}^T \mathbf{\Phi}_{3i}$ will be canceled in the next step. From (4), we know that the computable terms $\dot{x}_{ri}, \dot{y}_{ri}$, and $\dot{\psi}_{ri}$ include, respectively, the leader's velocities $\dot{x}_{i-1}, \dot{y}_{i-1}$, and $\dot{\psi}_{i-1}$. When we employ the backstepping design procedure to construct the actual controller $\boldsymbol{\tau}_i$, the differentiation of the virtual control inputs (26)–(28) will be utilized in the actual controller. Note that the derivatives of virtual control inputs (26)–(28) will include the leader's accelerations $\ddot{x}_{i-1}$, $\ddot{y}_{i-1}$, and $\ddot{\psi}_{i-1}$. However, the vehicle's accelerations are often directly unmeasurable, since a surface vehicle is typically equipped without any sensor for vehicle's accelerations in the practical applications. Without using vehicle's accelerations, we introduce the DSC technique in our control design. Let $\boldsymbol{\alpha}_{mi}$ pass through the following first-order filter to obtain $\boldsymbol{\alpha}_{fi}$:

$$\boldsymbol{\mu}_i \dot{\boldsymbol{\alpha}}_{fi} + \boldsymbol{\alpha}_{fi} = \boldsymbol{\alpha}_{mi},\ \boldsymbol{\alpha}_{fi}(0) = \boldsymbol{\alpha}_{mi}(0) \tag{30}$$

where $\boldsymbol{\mu}_i = \mathrm{diag}[\mu_{1i}, \mu_{2i}, \mu_{3i}]$ is the filter time constants and $\boldsymbol{\alpha}_{mi} = \boldsymbol{\alpha}_i - \boldsymbol{\mu}_i \mathbf{\Phi}_{3i}$. The derivative of $\boldsymbol{\alpha}_{fi}$ can be obtained from the filter (30) without using the accelerations of the leader. From (23) and (30), the derivative of $\mathbf{e}_{\boldsymbol{\alpha}_i}$ is

$$\dot{\mathbf{e}}_{\boldsymbol{\alpha}_i} = -\boldsymbol{\mu}_i^{-1} \mathbf{e}_{\boldsymbol{\alpha}_i} - \mathbf{\Phi}_{3i} - \mathbf{B}_i(\cdot) \tag{31}$$

where $\mathbf{e}_{\boldsymbol{\alpha}_i} = [e_{\alpha_{1i}}, e_{\alpha_{2i}}, e_{\alpha_{3i}}]^T$, $\boldsymbol{\mu}_i^{-1} = \mathrm{diag}[1/\mu_{1i}, 1/\mu_{2i}, 1/\mu_{3i}]$, and $\mathbf{B}_i(\cdot) = [B_{1i}(\cdot), B_{2i}(\cdot), B_{3i}(\cdot)]^T \triangleq \dot{\boldsymbol{\alpha}}_i$, in which $B_{1i}(\boldsymbol{\eta}_{ri}, \dot{\boldsymbol{\eta}}_{ri}, \ddot{\boldsymbol{\eta}}_{ri}, \underline{e}_{ji}, \dot{\underline{e}}_{ji}, \ddot{\underline{e}}_{ji}, \overline{e}_{ji}, \dot{\overline{e}}_{ji}, \ddot{\overline{e}}_{ji}, z_{ji}, \mathbf{z}_{2i}, \mathbf{e}_{\boldsymbol{\alpha}_i})$, B_{2i} $(\boldsymbol{\eta}_{ri}, \dot{\boldsymbol{\eta}}_{ri}, \ddot{\boldsymbol{\eta}}_{ri}, \underline{e}_{ji}, \dot{\underline{e}}_{ji}, \ddot{\underline{e}}_{ji}, \overline{e}_{ji}, \dot{\overline{e}}_{ji}, \ddot{\overline{e}}_{ji}, z_{ji}, \mathbf{z}_{2i}, \mathbf{e}_{\boldsymbol{\alpha}_i})$, and $B_{3i}(\psi_{ri}, \dot{\psi}_{ri}, \ddot{\psi}_{ri}, \underline{e}_{\psi i}, \dot{\underline{e}}_{\psi i}, \ddot{\underline{e}}_{\psi i}, \overline{e}_{\psi i}, \dot{\overline{e}}_{\psi i}, \ddot{\overline{e}}_{\psi i}, z_{\psi i}, z_{23i}, e_{\alpha_{3i}})$ are continuous functions according to (26)–(28).

Consider the Lyapunov function candidate $V_{1i} = V_{0i} + \frac{1}{2}\sum_{l=1}^{3} e_{\alpha_{li}}^2$, whose derivative along (29)–(31) is

$$\dot{V}_{1i} = -k_{z_{xi}} z_{xi}^2 - k_{z_{yi}} z_{yi}^2 - k_{z_{\psi i}} z_{\psi i}^2 - \sum_{l=1}^{3} \frac{e_{\alpha_{li}}^2}{\mu_{li}} + \mathbf{z}_{2i}^T \mathbf{\Phi}_{3i} - \sum_{l=1}^{3} e_{\alpha_{li}} B_{li}(\cdot). \tag{32}$$

Step 2: Differentiating (22) along (2), (30), and (23), and multiplying by the inertia matrix $\mathbf{M}_i$, we obtain

$$\mathbf{M}_i \dot{\mathbf{z}}_{2i} = -\mathbf{C}(\boldsymbol{\nu}_i)\boldsymbol{\nu}_i - \mathbf{D}(\boldsymbol{\nu}_i)\boldsymbol{\nu}_i + \boldsymbol{\tau}_i + \boldsymbol{\tau}_{wi} + \mathbf{M}_i(\boldsymbol{\mu}_i^{-1}\mathbf{e}_{\boldsymbol{\alpha}_i} + \mathbf{\Phi}_{3i}). \tag{33}$$

From system (2), we know that the terms $\mathbf{C}(\boldsymbol{\nu}_i)\boldsymbol{\nu}_i$ and $\mathbf{M}_i(\boldsymbol{\mu}_i^{-1}\mathbf{e}_{\boldsymbol{\alpha}_i} + \mathbf{\Phi}_{3i})$ are partially known, and they could be rewritten as the product of unknown constant parameters and known functions, namely, parametric uncertainties. Thus, substituting (3) into (33) yields

$$\mathbf{M}_i \dot{\mathbf{z}}_{2i} = \mathbf{G}_i \Theta_i - \mathbf{D}(\boldsymbol{\nu}_i)\boldsymbol{\nu}_i + \boldsymbol{\tau}_{wi} + \boldsymbol{\tau}_i \tag{34}$$

with

$$\mathbf{G}_i = \begin{bmatrix} G_{11i} & v_i r_i & r_i^2 & 0 \\ -u_i r_i & G_{22i} & G_{23i} & 0 \\ u_i v_i & -u_i v_i & G_{33i} & G_{34i} \end{bmatrix}$$

$$G_{11i} = \mu_{1i}^{-1} e_{\alpha_{1i}} + z_{xi} p_{xi}\cos\psi_i + z_{yi} p_{yi}\sin\psi_i$$

$$G_{22i} = \mu_{2i}^{-1} e_{\alpha_{2i}} + z_{yi} p_{yi}\cos\psi_i - z_{xi} p_{xi}\sin\psi_i$$

$$G_{23i} = \mu_{3i}^{-1} e_{\alpha_{3i}} + z_{\psi i} p_{\psi i}$$

$$G_{33i} = -u_i r_i + \mu_{2i}^{-1} e_{\alpha_{2i}} + z_{yi} p_{yi}\cos\psi_i - z_{xi} p_{xi}\sin\psi_i$$

$$G_{34i} = \mu_{3i}^{-1} e_{\alpha_{3i}} + z_{\psi i} p_{\psi i}$$

$$\Theta_i = [m_{11i}, m_{22i}, m_{23i}, m_{33i}]^T \tag{35}$$

where $\mathbf{G}_i$ is a known function matrix and Θ_i is an unknown constant vector. It is interesting to notice that system (34) includes both known and unknown information, and both parametric and nonparametric uncertainties, and is subject to the external disturbance $\boldsymbol{\tau}_{wi}$. The known information represented by $\mathbf{G}_i$ is available through the physics laws. The unknown constant vector Θ_i and the unknown nonlinear dynamics $\mathbf{D}(\boldsymbol{\nu}_i)$ come from the inaccurately modeling and modeling reduction. Note that the time-varying disturbance $\boldsymbol{\tau}_{wi}$ is bounded by unknown positive constants according to Assumption 1; thus, the disturbance $\boldsymbol{\tau}_{wi}$ could be compensated by estimating its upper bound. In what follows, the unknown positive constants $\bar{\tau}_{wli}, l = 1, 2, 3$, and unknown constant vector Θ_i are solved using model-based adaptive control techniques, and the unknown nonlinear function $\mathbf{D}(\boldsymbol{\nu}_i)\boldsymbol{\nu}_i$ is approximated by NNs [42]–[44]. Let

$$\mathbf{F}_i(Z_i) = \mathbf{D}(\boldsymbol{\nu}_i)\boldsymbol{\nu}_i \tag{36}$$

where $\mathbf{F}_i(Z_i) = [f_{1i}(Z_i), f_{2i}(Z_i), f_{3i}(Z_i)]^T \in R^3$, $Z_i = \boldsymbol{\nu}_i \in \Omega_{Z_i} \subset R^3$, with Ω_{Z_i} being a known compact set. By employing the universal approximation of Gaussian radial basis function (RBF) NNs [42], the continuous functions $f_{li}(Z_i)$, $l = 1, 2, 3$, could be expressed as

$$f_{li}(Z_i) = W_{li}^{*T} S_{li}(Z_i) + \epsilon_{li}(Z_i), \quad l = 1, 2, 3 \tag{37}$$

where W_{li}^* denotes the ideal constant weight vector, $\epsilon_{li}(Z_i)$ is the approximation error satisfying $|\epsilon_{li}| < \epsilon_{li}^*$ with constant $\epsilon_{li}^* > 0$, and $S_{li}(Z_i)$ is the Gaussian RBF vector [42] satisfying $\|S_{li}(Z_i)\| \le s_{li}^*$ with constant $s_{li}^* > 0$.

For system (34), the feedback control law $\boldsymbol{\tau}_i$ could be taken as

$$\boldsymbol{\tau}_i = -\mathbf{K}_{2i}\mathbf{z}_{2i} - \mathbf{G}_i\hat{\Theta}_i + \hat{\mathbf{W}}_i^T\mathbf{S}_i(Z_i) - \hat{\bar{\boldsymbol{\tau}}}_{wi} - \boldsymbol{\Phi}_{3i} \quad (38)$$

where $\mathbf{K}_{2i} = \mathrm{diag}[k_{21i}, k_{22i}, k_{23i}] > 0$ is design parameters, $\hat{\mathbf{W}}_i^T \triangleq \mathrm{blockdiag}\{\hat{W}_{1i}^T, \hat{W}_{2i}^T, \hat{W}_{3i}^T\}$, $\mathbf{S}_i(Z_i) = [S_{1i}^T(Z_i), S_{2i}^T(Z_i), S_{3i}^T(Z_i)]^T$, and

$$\hat{\bar{\boldsymbol{\tau}}}_{wi} = \begin{bmatrix} \hat{\bar{\tau}}_{w1i}\tanh(\frac{z_{21i}\hat{\bar{\tau}}_{w1i}}{\zeta}) \\ \hat{\bar{\tau}}_{w2i}\tanh(\frac{z_{22i}\hat{\bar{\tau}}_{w2i}}{\zeta}) \\ \hat{\bar{\tau}}_{w3i}\tanh(\frac{z_{23i}\hat{\bar{\tau}}_{w3i}}{\zeta}) \end{bmatrix}$$

with $\tanh(\cdot)$ being a *hyperbolic tangent* function and $\zeta > 0$ being a design parameter, in which $\hat{\Theta}_i$ is the estimate of Θ_i, $\hat{W}_{li}$ is the estimate of the W_{li}^*, and $\hat{\bar{\boldsymbol{\tau}}}_{wi}$ is the estimate of the $\bar{\tau}_{wli}$, $l = 1, 2, 3$. Throughout this paper, we denote the estimate error as $\tilde{(\cdot)} = \hat{(\cdot)} - (\cdot)$. Consider the following adaptation laws:

$$\begin{aligned} \dot{\hat{W}}_{li} &= \boldsymbol{\Gamma}_{li}\left(S_{li}(Z_i)z_{2li} - \sigma_{li}\hat{W}_{li}\right) \\ \dot{\hat{\Theta}}_i &= \boldsymbol{\Gamma}_{\Theta i}\left(\mathbf{G}_i^T\mathbf{z}_{2i} - \sigma_i\hat{\Theta}_i\right) \\ \dot{\hat{\bar{\tau}}}_{wli} &= \Gamma_{wli}(|z_{2li}| - \sigma_{wli}\hat{\bar{\tau}}_{wli}), \qquad l = 1, 2, 3 \end{aligned} \quad (39)$$

where $\boldsymbol{\Gamma}_{li} = \boldsymbol{\Gamma}_{li}^T > 0$ and $\boldsymbol{\Gamma}_{\Theta i} = \boldsymbol{\Gamma}_{\Theta i}^T > 0, \Gamma_{wli} > 0$ are the designed adaptation gains, and $\sigma_{li} > 0$, $\sigma_i > 0$, and $\sigma_{wli} > 0$ are the σ-modification parameters.

Next, we present the proposed adaptive formation control that ensures the uniformly ultimate boundedness (UUB) of the closed-loop system and guarantees the prescribed performance of formation tracking errors.

Theorem 1: Under Assumptions 1–3, consider N USVs with dynamics (1) and (2) and control input $\boldsymbol{\tau}_i$ given in (38) with adaptation law (39). Assume that there exists a sufficiently large compact set $\Omega_{Z_i} \subset R^3$ such that $Z_i \in \Omega_{Z_i}$ for all $t \geq 0$. If given any $\varsigma_i > 0$ for all initial conditions satisfying $V_{2i}(0) \leq \varsigma_i$, then there exist design parameters $k_{z_{xi}}$, $k_{z_{yi}}$, $k_{z_{\psi i}}$, μ_{li}, $l = 1, 2, 3$, κ_i, $\boldsymbol{\Gamma}_{\Theta i}$, $\boldsymbol{\Gamma}_{li}$, Γ_{wli}, and $\mathbf{K}_{2i}$, such that $V_{2i}(t) \leq \varsigma_i\ \forall t > 0$ and $\dot{V}_{2i} \leq -\rho_i V_{2i} + \delta_i$ hold, which mean that:

i) the tracking errors $e_{ji}(t)$ ultimately converge to a small neighborhood around zero, whose size could be adjusted by tuning the design parameters;
ii) all the signals in the closed-loop system are uniformly ultimately bounded;
iii) the prescribed performance of tracking errors $e_{ji}(t)$ in the sense of (8) and (9) is guaranteed;
iv) each vehicle and its leader are *collision-free*, i.e., $e_{zi}(t) < d_i - \underline{d}_i, \forall t \geq 0, i = 2, 3, ..., N$, when the maximum values of function (9) satisfying (10).

Proof: (i) Consider the following Lyapunov function:

$$V_{2i} = V_{1i} + \frac{1}{2}\mathbf{z}_{2i}^T\mathbf{M}_i\mathbf{z}_{2i} + \frac{1}{2}\tilde{\Theta}_i^T\boldsymbol{\Gamma}_{\Theta i}^{-1}\tilde{\Theta}_i + \frac{1}{2}\sum_{l=1}^{3}\tilde{W}_{li}^T\boldsymbol{\Gamma}_{li}^{-1}\tilde{W}_{li} + \frac{1}{2\Gamma_{wli}}\sum_{l=1}^{3}\tilde{\bar{\tau}}_{wli}^2 \quad (40)$$

whose derivative along (34), (39), (38), and (32) is

$$\begin{aligned} \dot{V}_{2i} = & -k_{z_{xi}}z_{xi}^2 - k_{z_{yi}}z_{yi}^2 - k_{z_{\psi i}}z_{\psi i}^2 - \sum_{l=1}^{3}\frac{e_{\alpha_{li}}^2}{\mu_{li}} \\ & - \mathbf{z}_{2i}^T\mathbf{K}_{2i}\mathbf{z}_{2i} - \sum_{l=1}^{3}e_{\alpha_{li}}B_{li}(\cdot) - \sigma_i\tilde{\Theta}_i^T\hat{\Theta}_i \\ & - \sum_{l=1}^{3}\left(\sigma_{li}\tilde{W}_{li}^T\hat{W}_{li} + \sigma_{wli}\tilde{\bar{\tau}}_{wli}\hat{\bar{\tau}}_{wli}\right) - \mathbf{z}_{2i}^T\boldsymbol{\epsilon}_i(Z_i) \\ & + \sum_{l=1}^{3}\left(z_{2li}\tau_{wli} - |z_{2li}|\bar{\tau}_{wli} + |z_{2li}|\hat{\bar{\tau}}_{wli}\right. \\ & \left. - z_{2li}\hat{\bar{\tau}}_{wli}\tanh\frac{z_{2li}\hat{\bar{\tau}}_{wli}}{\zeta}\right) \end{aligned} \quad (41)$$

where $\boldsymbol{\epsilon}_i(Z_i) = [\epsilon_{1i}(Z_i), \epsilon_{2i}(Z_i), \epsilon_{3i}(Z_i)]^T$. Using Assumption 1, we have the inequality $z_{2li}\tau_{wli} \leq |z_{2li}|\bar{\tau}_{wli}$, and note the fact that $|z_{2li}|\hat{\bar{\tau}}_{wli} \leq |z_{2li}\hat{\bar{\tau}}_{wli}|$. Note that the hyperbolic tangent function $\tanh(\cdot)$ has the following property [45]:

$$0 \leq |a| - a\tanh\left(\frac{a}{\zeta}\right) \leq \kappa_p\zeta, \quad \kappa_p = 0.2785$$

for any $\zeta > 0$ and $a \in R$, which yields

$$\sum_{l=1}^{3}\left(z_{2li}\tau_{wli} - |z_{2li}|\bar{\tau}_{wli} + |z_{2li}|\hat{\bar{\tau}}_{wli} - z_{2li}\hat{\bar{\tau}}_{wli}\tanh\frac{z_{2li}\hat{\bar{\tau}}_{wli}}{\zeta}\right) \leq 3\kappa_p\zeta.$$

Consider the compact sets $\Omega_{di} := \{(\|\boldsymbol{\eta}_{ri}\|^2 + \|\dot{\boldsymbol{\eta}}_{ri}\|^2 + \|\ddot{\boldsymbol{\eta}}_{ri}\|^2 + \underline{e}_{ji}^2 + \underline{\dot{e}}_{ji}^2 + \underline{\ddot{e}}_{ji}^2 + \bar{e}_{ji}^2 + \dot{\bar{e}}_{ji}^2 + \ddot{\bar{e}}_{ji}^2) \leq B_{di}\}$ and $\Omega_i := \{(z_{ji}^2 + \|\mathbf{e}_{\alpha_i}\|^2 + \|\mathbf{z}_{2i}\|^2 + \|\tilde{\Theta}_i\|^2 + \|\tilde{W}_{li}\|^2 + \tilde{\bar{\tau}}_{wli}^2) \leq 2\varsigma_i\}$ with constants $B_{di} > 0$ and $\varsigma_i > 0$. From (31), we know that the continuous function $B_{li}(\cdot)$, $l = 1, 2, 3$, are bounded on the compact set $\Omega_{di} \times \Omega_i$ by applying the continuous property, that is, $B_{li}(\cdot)$ satisfy $|B_{li}(\cdot)| \leq \bar{B}_{li}$ on the compact set $\Omega_{di} \times \Omega_i$, with $\bar{B}_{li}$ being positive constants. By completion of squares,

we have

$$-e_{\alpha_{li}} B_{li}(\cdot) \le \frac{\kappa_i e_{\alpha_{li}}^2}{2} + \frac{\bar{B}_{li}^2}{2\kappa_i}$$

$$-\sigma_i \tilde{\Theta}_i^T \hat{\Theta}_i \le -\frac{\sigma_i \|\tilde{\Theta}_i\|^2}{2} + \frac{\sigma_i \|\Theta_i\|^2}{2}$$

$$-\sigma_{li} \tilde{W}_{li}^T \hat{W}_{li} \le -\frac{\sigma_{li} \|\tilde{W}_{li}\|^2}{2} + \frac{\sigma_{li} \|W_{li}^*\|^2}{2}$$

$$-\sigma_{wli} \tilde{\bar{\tau}}_{wli} \hat{\bar{\tau}}_{wli} \le -\frac{\sigma_{wli} \tilde{\bar{\tau}}_{wli}^2}{2} + \frac{\sigma_{wli} \bar{\tau}_{wli}^2}{2}$$

$$-\mathbf{z}_{2i}^T \boldsymbol{\epsilon}_i(Z_i) \le \frac{\kappa_i \|\mathbf{z}_{2i}\|^2}{2} + \frac{1}{2\kappa_i} \sum_{l=1}^{3} \epsilon_{li}^{*2}$$

with constant $\kappa_i > 0$. Thus, we have

$$\dot{V}_{2i} \le -\rho_i V_{2i} + \delta_i \tag{42}$$

in which

$$\delta_i = \frac{\sigma_i \|\Theta_i\|^2}{2} + \sum_{l=1}^{3} \left(\frac{\bar{B}_{li}^2 + \epsilon_{li}^{*2}}{2\kappa_i} + \frac{\sigma_{li} \|W_{li}^*\|^2 + \sigma_{wli} \bar{\tau}_{wli}^2}{2} \right) + 3\kappa_p \zeta$$

$$\rho_i = \min \left\{ 2k_{z_{xi}}, 2k_{z_{yi}}, 2k_{z_{\psi i}}, \frac{2}{\mu_{li}} - \kappa_i, \frac{\lambda_{\min}(2\mathbf{K}_{2i} - \kappa_i I_3)}{\lambda_{\max}(\mathbf{M}_i)}, \frac{\sigma_i}{\lambda_{\max}(\boldsymbol{\Gamma}_{\Theta i}^{-1})}, \frac{\sigma_{li}}{\lambda_{\max}(\boldsymbol{\Gamma}_{li}^{-1})}, \sigma_{wli} \Gamma_{wli} \right\}$$

where I_3 denotes the identity matrix, and $\lambda_{\min}(\bullet)$ and $\lambda_{\max}(\bullet)$ denote the minimum and maximum eigenvalue of the symmetric matrix, respectively. For choosing $\rho_i > \delta_i/\varsigma_i$, we have $\dot{V}_{2i} \le 0$ on $V_{2i} = \varsigma_i$. Therefore, $V_{2i} \le \varsigma_i$ is an invariant set, i.e., if $V_{2i}(0) \le \varsigma_i$, then $V_{2i}(t) \le \varsigma_i$ for all $t > 0$. Inequality (42) implies that

$$V_{2i}(t) \le V_{2i}(0) \exp(-\rho_i t) + \varrho_i \le c_{0i} \quad \forall t \ge 0 \tag{43}$$

where $\varrho_i = \delta_i/\rho_i$ and $c_{0i} = V_{2i}(0) + \varrho_i$. From (40) and (43) as t tends to infinity, we have

$$|z_{ji}| \le \sqrt{2\varrho_i}, \quad |e_{\alpha_{li}}| \le \sqrt{2\varrho_i}, \quad \|\mathbf{z}_{2i}\| \le \sqrt{2\varrho_i/\lambda_{\min}(\mathbf{M}_i)},$$
$$\|\tilde{\Theta}_i\| \le \sqrt{2\varrho_i/\lambda_{\min}(\boldsymbol{\Gamma}_{\Theta i}^{-1})}, \quad \|\tilde{W}_{li}\| \le \sqrt{2\varrho_i/\lambda_{\min}(\boldsymbol{\Gamma}_{li}^{-1})},$$
$$|\tilde{\bar{\tau}}_{wli}| \le \sqrt{2\varrho_i \Gamma_{wli}}. \tag{44}$$

From (44), it is clear that z_{ji} converge exponentially to a small residual set $\sqrt{2\varrho_i}$, whose size could be adjusted by choosing appropriate parameters $k_{z_{xi}}$, $k_{z_{yi}}$, $k_{z_{\psi i}}$, μ_{li}, $\mathbf{K}_{2i}$, $\boldsymbol{\Gamma}_{\Theta i}$, $\boldsymbol{\Gamma}_{li}$, Γ_{wli}, σ_i, σ_{li}, and σ_{wli}. Using (11) and (13), we know that the tracking errors $e_{ji}(t)$ converge to an adjustable size of zero as z_{ji} converge to the adjustable residual set $\sqrt{2\varrho_i}$.

(ii) It follows from (44) that the error variables z_{ji}, $e_{\alpha_{li}}$, $\mathbf{z}_{2i}$, $\tilde{\Theta}_i$, $\tilde{W}_{li}$, and $\tilde{\bar{\tau}}_{wli}$ are uniformly ultimately bounded. Using (5), we have that the output of the system $\boldsymbol{\eta}_i$ is bounded. Subsequently, the boundedness of z_{ji} ensures the boundedness of virtual control $\boldsymbol{\alpha}_i$ in (26)–(28) and guarantees the boundedness of $\boldsymbol{\alpha}_{fi}$ in (23), which yields bounded state $\boldsymbol{\nu}_i$ by the error coordinate transformation (22). Since $\tilde{\Theta}_i = \hat{\Theta}_i - \Theta_i$ and Θ_i in (35) is bounded, we obtain that $\hat{\Theta}_i$ is bounded. Similarly, the boundedness of $\hat{W}_{li}$ and $\hat{\bar{\tau}}_{wli}$ could be guaranteed by the boundedness of $\tilde{W}_{li}$, W_{li}^*, $\tilde{\bar{\tau}}_{wli}$, and $\bar{\tau}_{wli}$. Thus, we can conclude that the feedback control law $\boldsymbol{\tau}_i$ in (38) is also bounded, and then, all the signals in the closed-loop system are uniformly ultimately bounded.

(iii) From (40) and (43), we have $\frac{1}{2} z_{ji}^2 \le V_{2i}(0) \exp(-\rho_i t) + \varrho_i \le c_{0i}$, which yields

$$|z_{ji}| \le \sqrt{2c_{0i}}. \tag{45}$$

From (13) and (12), we have

$$\frac{e_{ji}}{\bar{e}_{ji}} = T_{ji}(\cdot) = \frac{1 - e^{-2z_{ji}}}{1 + \gamma_{ji}^{-1} e^{-2z_{ji}}}. \tag{46}$$

Using inequality (45), we have the lower bound $z_{ji} = -\sqrt{2c_{0i}}$ and the upper bound $z_{ji} = \sqrt{2c_{0i}}$. Note the monotonicity of $T_{ji}(\cdot)$ in (46) with respect to z_{ji}, and thus, we have

$$\frac{1 - e^{2\sqrt{2c_{0i}}}}{1 + \gamma_{ji}^{-1} e^{2\sqrt{2c_{0i}}}} \le \frac{e_{ji}}{\bar{e}_{ji}} \le \frac{1 - e^{-2\sqrt{2c_{0i}}}}{1 + \gamma_{ji}^{-1} e^{-2\sqrt{2c_{0i}}}} \quad \forall t \ge 0. \tag{47}$$

It is easy to verify that $-\gamma_{ji} < \frac{1-e^{2\sqrt{2c_{0i}}}}{1+\gamma_{ji}^{-1} e^{2\sqrt{2c_{0i}}}}$ and $\frac{1-e^{-2\sqrt{2c_{0i}}}}{1+\gamma_{ji}^{-1} e^{-2\sqrt{2c_{0i}}}} < 1$. Hence, (47) indicates that $-\gamma_{ji} < \frac{e_{ji}}{\bar{e}_{ji}} < 1$, which yields $-\underline{e}_{ji}(t) < e_{ji} < \bar{e}_{ji}$. That is, the prescribed performance of tracking errors $e_{ji}(t)$ in the sense of (8) and (9) is guaranteed.

(iv) The prescribed performance of tracking errors $e_{ji}(t)$ in the sense of (8) and (9) has been guaranteed by step (iii). If the maximum values of function (9) satisfy (10), then we apply Corollary 1 to obtain that each vehicle and its leader are collision-free, i.e., $e_{zi}(t) < d_i - \underline{d}_i, \forall t \ge 0, i = 2, 3, ..., N$. This completes the proof.

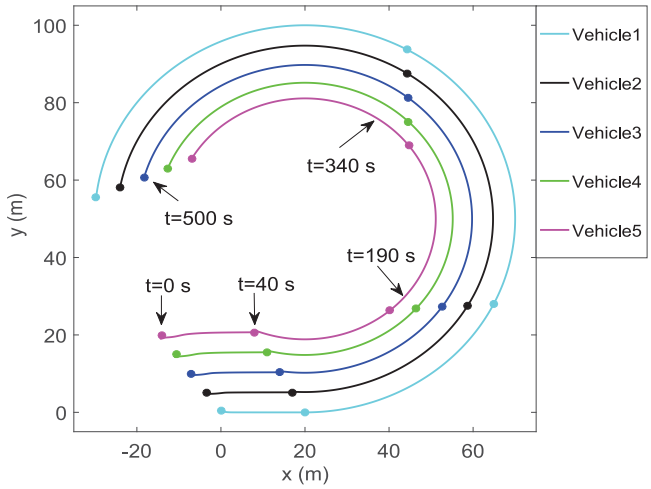

Fig. 2. Phase–plane trajectories of five vehicles and their snapshots at several key time instants.

IV. Simulation Studies

In this section, simulation studies are performed on five, i.e., $N = 5$, identical vehicles with system parameters taken

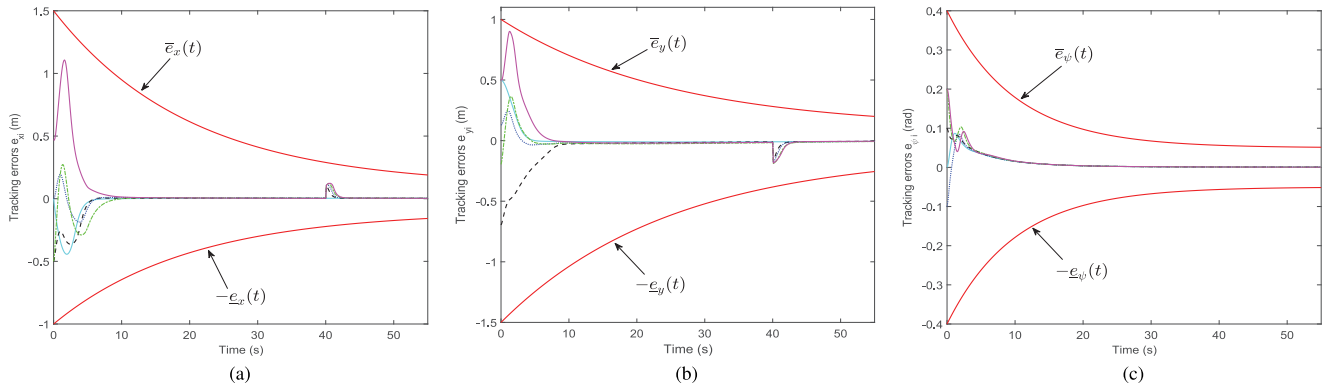

Fig. 3. Evolution of the tracking errors. (a) Evolution of x-direction tracking errors $e_{xi}(t)$, along with the performance functions $-\underline{e}_x(t)$ and $\overline{e}_x(t)$. (b) Evolution of y-direction tracking errors $e_{yi}(t)$, along with the performance functions $-\underline{e}_y(t)$ and $\overline{e}_y(t)$. (c) Evolution of the yaw angle tracking errors $e_{\psi i}$, along with the performance functions $-\underline{e}_\psi(t)$ and $\overline{e}_\psi(t)$.

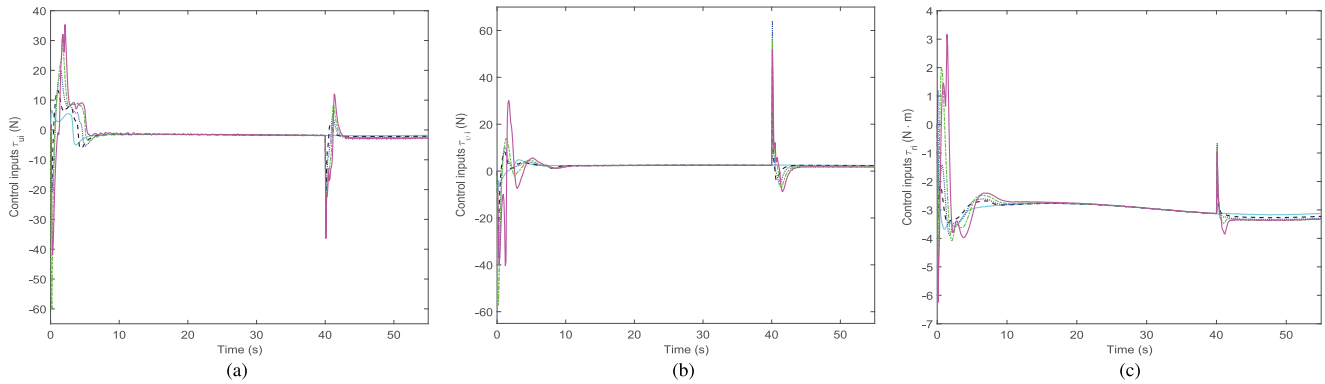

Fig. 4. Control inputs. (a) Surge forces τ_{ui}. (b) Sway forces τ_{vi}. (c) Yaw moments τ_{ri}.

from [38]. The length of the vehicle is 1.255 m, and the mass parameters are $m_{11} = 25.8$ kg, $m_{22} = 33.8$ kg, $m_{23} = 1.0948$ kg, and $m_{33} = 2.76$ kg. The damping terms are given by $d_{11} = 0.7225 + 1.3274|u| + 5.8664u^2$, $d_{22} = 0.8612 + 36.2823|v| + 0.805|r|$, $d_{23} = -0.1079 + 0.845|v| + 3.45|r|$, $d_{32} = -0.1052 - 5.0437|v| - 0.13|r|$, and $d_{33} = 1.9 - 0.08|v| + 0.75|r|$. The external disturbances are $\boldsymbol{\tau}_{wi} = [3 - 0.2\sin(0.1t) + 0.1\cos(0.02t) + 0.1\text{rand}(\cdot), -2.5 + 0.1\cos(0.1t) + 0.1\sin(0.02t) + 0.1\text{rand}(\cdot), 3 - 0.2\sin(0.1t) - 0.1\cos(0.02t) + 0.1\text{rand}(\cdot)]^T$, where $\text{rand}(\cdot) \in [0, 1]$ returns quasi-random value denoting the random noise.

The formation control objective is to guarantee that the five identical vehicles track their reference trajectories to establish and maintain the parallel straight-line and circle formation pattern with guaranteeing prescribed performances and collision avoidance. The reference trajectory consisting of a straight line and a circle is given by

$$\begin{cases} \boldsymbol{\eta}_0 = [0.5t, 0, 0]^T, & \text{if } t \le t_c \\ \boldsymbol{\eta}_0 = [0.5t_c + 50\sin t', 50(1 - \cos t'), t']^T, & \text{if } t > t_c \end{cases} \tag{48}$$

with $t' = 0.01(t - t_c)$ and the time constant $t_c \ge 0$. The desired prescribed performance functions are chosen as $\overline{e}_x(t) = \overline{e}_{xi}(t) = (1.5 - 0.1)\exp(-0.05t) + 0.1$, $\underline{e}_x(t) = \underline{e}_{xi}(t) = (1 - 0.1)\exp(-0.05t) + 0.1$, $\overline{e}_y(t) = \overline{e}_{yi}(t) = (1 - 0.1)\exp(-0.04t) + 0.1$, $\underline{e}_y(t) = \underline{e}_{yi}(t) = (1.5 - 0.1)\exp(-0.04t) + 0.1$, and $\overline{e}_\psi(t) = \underline{e}_\psi(t) = \overline{e}_{\psi i}(t) = \underline{e}_{\psi i}(t) = (0.4 - 0.05)\exp(-0.1t) + 0.05$.

We apply the proposed formation controller (38) with adaptation law (39) to achieve the above formation control objective. The desired distance, the relative heading angle, and the desired angle between the leading vehicle 1 and the reference trajectory are $d_1 = 0$, $\beta_1 = 0$, and $\theta_1 = 0$, respectively. Let $t_c = 40$ s, the safety distance $\underline{d}_i = 3.5$ m, the relative heading angle $\beta_i = 0$, and the desired angle $\theta_i = \frac{2\pi}{3}$, $i = 2, 3, 4, 5$. To illustrate that formation controller (38) could be also applicable to the time-varying formation, the design parameter d_i $(i = 2, 3, 4, 5)$ is chosen as time-varying parameter, i.e., $d_i = 6$ when $t \le t_c$ and $d_i = 6.2$ when $t > t_c$. By time-varying formation, we mean that one or more of the design parameters d_i, β_i, and θ_i are time-varying. The time-varying formation could be utilized to accomplish different missions.

After carefully considering the unknown dynamics $\mathbf{D}(\boldsymbol{\nu}_i)\boldsymbol{\nu}_i$ with the above damping terms, we have the NN inputs $Z_{1i} = u_i$ and $Z_{2i} = Z_{3i} = [v_i, r_i]^T$. Thus, we construct the Gaussian RBF NNs $\hat{W}_{1i}^T S_{1i}(Z_{1i})$ using 24 nodes, with the width 0.45 and the centers evenly spaced on $[-0.9, 1.2]$; $\hat{W}_{2i}^T S_{2i}(Z_{2i})$ using 49 nodes, with the width 0.45 and the centers evenly spaced on $[-0.9, 0.9] \times [-0.9, 0.9]$; and $\hat{W}_{3i}^T S_{3i}(Z_{3i})$ using 49 nodes, with the width 0.45 and the centers evenly spaced on $[-1.2, 1.2] \times [-1.2, 1.2]$. The design parameters are taken as $k_{z_{x1}} = k_{z_{x2}} = k_{z_{x3}} = k_{z_{y1}} = k_{z_{y2}} = k_{z_{y3}} = k_{z_{\psi i}} = 1$, $k_{z_{x4}} =$

$k_{z_{x5}} = k_{z_{y4}} = k_{z_{y5}} = 0.5$, $\mathbf{K}_{21} = \mathbf{K}_{22} = \mathbf{K}_{23} = \text{diag}[2, 2, 2]$, $\mathbf{K}_{24} = \mathbf{K}_{25} = \text{diag}[1, 1, 1]$, $\boldsymbol{\mu}_i = \text{diag}[0.05, 0.05, 0.05]$, $\boldsymbol{\Gamma}_{\Theta i} = \text{diag}[2, 2, 2, 2]$, $\sigma_i = 0$, $\Gamma_{wli} = 4$, $\sigma_{wli} = 0$, $\zeta = 0.2$, $\boldsymbol{\Gamma}_{li} = \text{diag}[1, 1, 1]$, and $\sigma_{li} = \text{diag}[0.1, 0.01, 0.02]$, $l = 1, 2, 3$, $i = 1, 2, 3, 4, 5$. The initial conditions are $\hat{\Theta}_i(0) = [10, 20, 1, 2]^T$, $\hat{\bar{\tau}}_{wli}(0) = 2$, $\boldsymbol{\eta}_1(0) = [0, 0.5, 0]^T$, $\boldsymbol{\eta}_2(0) = [-3.5, 5, 0]^T$, $\boldsymbol{\eta}_3(0) = [-7, 10, 0]^T$, $\boldsymbol{\eta}_4(0) = [-10.5, 15, 0.2]^T$, $\boldsymbol{\eta}_5(0) = [-14, 20, 0.4]^T$, $\boldsymbol{\nu}_i(0) = [0, 0, 0]^T$, and zero initial NN weight estimates.

Simulation results are presented in Figs. 2–4. Fig. 2 displays the phase–plane trajectories of five vehicles and their snapshots at 0, 40, 190, 340, and 500 s. The tracking errors $e_{ji}(t)$, along with the prescribed boundary functions $\bar{e}_j(t)$ and $-\underline{e}_j(t)$, shown in Fig. 3(a)–(c), converge to a small neighborhood of zero without violation of the prescribed performance bounds. Despite the presence of modeling uncertainties and external time-varying disturbances, the tracking errors depicted in Fig. 3(a)–(c) illustrate that the prescribed performance constraints on the tracking errors are satisfied using the proposed adaptive formation controller. Note that the reference trajectory (48) switches from the straight line to the circle, and the design parameter d_i $(i = 2, 3, 4, 5)$ jumps from 6 to 6.2 at the switching instant $t = 40$ s. Thus, the tracking errors change abruptly at the switching instant, but the tracking errors still remain within the prescribed feasible regions, as shown in Fig. 3(a) and (b). The evolution of the tracking errors shown in Fig. 3(a) and (b) indicates that the position tracking error $z_i(t)$ satisfies the collision-free condition (7) for the entire simulation time, which means each vehicle and its leader are collision-free. The control inputs $\boldsymbol{\tau}_i = [\tau_{ui}, \tau_{vi}, \tau_{ri}]^T$ are depicted in Fig. 4(a)–(c).

V. Conclusion

This paper presented decentralized leader–follower formation control with prescribed performance and collision avoidance for a group of fully actuated USVs subject to parametric and nonparametric uncertainties and external disturbances. Prescribed performance constraints on formation errors were considered in the feedback control design. By appropriately choosing the initial values of exponentially decaying functions and guaranteeing the prescribed performance, each vehicle and its leader are collision-free. Based on the DSC technique, the PPC methodology, the backstepping procedure, and the Lyapunov synthesis, a decentralized adaptive formation controller was designed such that UUB of the closed-loop system with prescribed performance was guaranteed, and the potential collision between each vehicle and its leader was avoided.

References

[1] R. Cui, Y. Li, and W. Yan, "Mutual information-based multi-AUV path planning for scalar field sampling using multidimensional RRT*," *IEEE Trans. Syst., Man, Cybern.: Syst.*, vol. 46, no. 7, pp. 993–1004, Jul. 2016.

[2] Z. Peng, J. Wang, and D. Wang, "Distributed maneuvering of autonomous surface vehicles based on neurodynamic optimization and fuzzy approximation," *IEEE Trans. Control Syst. Technol.*, vol. 26, no. 3, pp. 1083–1090, May 2018.

[3] T. Balch and R. C. Arkin, "Behavior-based formation control for multirobot teams," *IEEE Trans. Robot. Automat.*, vol. 14, no. 6, pp. 926–939, Dec. 1998.

[4] K. D. Do, "Formation control of multiple elliptical agents with limited sensing ranges," *Automatica*, vol. 48, no. 7, pp. 1330–1338, 2012.

[5] Y. Cao, W. Yu, W. Ren, and G. Chen, "An overview of recent progress in the study of distributed multi-agent coordination," *IEEE Trans. Ind. Informat.*, vol. 9, no. 1, pp. 427–438, Feb. 2013.

[6] Q. Zhang, L. Lapierre, and X. Xiang, "Distributed control of coordinated path tracking for networked nonholonomic mobile vehicles," *IEEE Trans. Ind. Informat.*, vol. 9, no. 1, pp. 472–484, Feb. 2013.

[7] C. Yuan, H. He, and C. Wang, "Cooperative deterministic learning-based formation control for a group of nonlinear uncertain mechanical systems," *IEEE Trans. Ind. Informat.*, 2018, doi: 10.1109/TII.2018.2792455, to be published.

[8] R. Cui, S. S. Ge, B. V. E. How, and Y. S. Choo, "Leader–follower formation control of underactuated autonomous underwater vehicles," *Ocean Eng.*, vol. 37, no. 17, pp. 1491–1502, 2010.

[9] Z. Peng, J. Wang, and D. Wang, "Distributed containment maneuvering of multiple marine vessels via neurodynamics-based output feedback," *IEEE Trans. Ind. Electron.*, vol. 64, no. 5, pp. 3831–3839, May 2017.

[10] X. Jin, "Fault tolerant finite-time leader–follower formation control for autonomous surface vessels with LOS range and angle constraints," *Automatica*, vol. 68, no. 6, pp. 228–236, 2016.

[11] Y. Liu, B. Xu, and Y. Ding, "Convergence analysis of cooperative braking control for interconnected vehicle systems," *IEEE Trans. Intell. Transp. Syst.*, vol. 18, no. 7, pp. 1894–1906, Jul. 2017.

[12] W. He, Z. Yin, and C. Sun, "Adaptive neural network control of a marine vessel with constraints using the asymmetric barrier Lyapunov function," *IEEE Trans. Cybern.*, vol. 47, no. 7, pp. 1641–1651, Jul. 2017.

[13] Z. Peng, D. Wang, Z. Chen, X. Hu, and W. Lan, "Adaptive dynamic surface control for formations of autonomous surface vehicles with uncertain dynamics," *IEEE Trans. Control Syst. Technol.*, vol. 21, no. 2, pp. 513–520, Mar. 2013.

[14] N. Wang, S. Lv, M. J. Er, and W. H. Chen, "Fast and accurate trajectory tracking control of an autonomous surface vehicle with unmodeled dynamics and disturbances," *IEEE Trans. Intell. Veh.*, vol. 1, no. 3, pp. 230–243, Sep. 2016.

[15] S.-L. Dai, S. He, H. Lin, and C. Wang, "Platoon formation control with prescribed performance guarantees for USVs," *IEEE Trans. Ind. Electron.*, vol. 65, no. 5, pp. 4237–4246, May 2018.

[16] Z. Peng, J. Wang, and D. Wang, "Containment maneuvering of marine surface vehicles with multiple parameterized paths via spatial-temporal decoupling," *IEEE/ASME Trans. Mechatronics*, vol. 22, no. 2, pp. 1026–1036, Apr. 2017.

[17] R. Cui, C. Yang, Y. Li, and S. Sharma, "Adaptive neural network control of AUVs with control input nonlinearities using reinforcement learning," *IEEE Trans. Syst., Man, Cybern.: Syst.*, vol. 47, no. 6, pp. 1019–1029, Jun. 2017.

[18] Y.-L. Wang and Q.-L. Han, "Network-based fault detection filter and controller coordinated design for unmanned surface vehicles in network environments," *IEEE Trans. Ind. Informat.*, vol. 12, no. 5, pp. 1753–1765, Oct. 2016.

[19] S.-L. Dai, C. Wang, and F. Luo, "Identification and learning control of ocean surface ship using neural networks," *IEEE Trans. Ind. Informat.*, vol. 8, no. 4, pp. 801–810, Nov. 2012.

[20] Y.-L. Wang and Q.-L. Han, "Network-based modelling and dynamic output feedback control for unmanned marine vehicles in network environments," *Automatica*, vol. 91, no. 5, pp. 43–53, 2018.

[21] C. P. Bechlioulis and G. A. Rovithakis, "Robust adaptive control of feedback linearizable MIMO nonlinear systems with prescribed performance," *IEEE Trans. Autom Control*, vol. 53, no. 9, pp. 2090–2099, Oct. 2008.

[22] M. Wang, C. Wang, P. Shi, and X. Liu, "Dynamic learning from neural control for strict-feedback systems with guaranteed predefined performance," *IEEE Trans. Neural Netw. Learn. Syst.*, vol. 27, no. 12, pp. 2564–2576, Dec. 2016.

[23] C. Yang, Y. Jiang, Z. Li, W. He, and C.-Y. Su, "Neural control of bimanual robots with guaranteed global stability and motion precision," *IEEE Trans. Ind. Informat.*, vol. 13, no. 3, pp. 1162–1171, Jun. 2017.

[24] C. Yang, X. Wang, L. Cheng, and H. Ma, "Neural-learning-based telerobot control with guaranteed performance," *IEEE Trans. Cybern.*, vol. 47, no. 10, pp. 3148–3159, Oct. 2017.

[25] M. Wang and A. Yang, "Dynamic learning from adaptive neural control of robot manipulators with prescribed performance," *IEEE Trans. Syst., Man, Cybern.: Syst.*, vol. 47, no. 8, pp. 2244–2255, Aug. 2017.

[26] S.-L. Dai, M. Wang, and C. Wang, "Neural learning control of marine surface vessels with guaranteed transient tracking performance," *IEEE Trans. Ind. Electron.*, vol. 63, no. 3, pp. 1717–1727, Mar. 2016.

[27] D. Swaroop, J. K. Hedrick, P. P. Yip, and J. C. Gerdes, "Dynamic surface control for a class of nonlinear systems," *IEEE Trans. Autom. Control*, vol. 45, no. 10, pp. 1893–1899, Oct. 2000.
[28] M. Wang, X. Liu, and P. Shi, "Adaptive neural control of pure-feedback nonlinear time-delay systems via dynamic surface technique," *IEEE Trans. Syst., Man, Cybern. B, Cybern.*, vol. 41, no. 6, pp. 1681–1692, Dec. 2011.
[29] L. Long and J. Zhao, "Decentralized adaptive neural output-feedback DSC for switched large-scale nonlinear systems," *IEEE Trans. Cybern.*, vol. 47, no. 4, pp. 908–919, Apr. 2017.
[30] C. Chen, C. Wen, Z. Liu, K. Xie, Y. Zhang, and C. L. P. Chen, "Adaptive consensus of nonlinear multi-agent systems with non-identical partially unknown control directions and bounded modelling errors," *IEEE Trans. Autom. Control*, vol. 62, no. 9, pp. 4654–4659, Sep. 2017.
[31] C. Chen, C. Wen, Z. Liu, K. Xie, Y. Zhang, and C. P. Chen, "Adaptive asymptotic control of multivariable systems based on a one-parameter estimation approach," *Automatica*, vol. 83, no. 9, pp. 124–132, 2017.
[32] C. Yang, Y. Jiang, W. He, J. Na, Z. Li, and B. Xu, "Adaptive parameter estimation and control design for robot manipulators with finite-time convergence," *IEEE Trans. Ind. Electron.*, vol. 65, no. 10, pp. 8112–8123, Oct. 2018, doi: 10.1109/TIE.2018.2803773.
[33] W. He, Y. Ouyang, and J. Hong, "Vibration control of a flexible robotic manipulator in the presence of input deadzone," *IEEE Trans. Ind. Informat.*, vol. 13, no. 1, pp. 48–59, Feb. 2017.
[34] F. Wang, B. Chen, C. Lin, J. Zhang, and X. Meng, "Adaptive neural network finite-time output feedback control of quantized nonlinear systems," *IEEE Trans. Cybern.*, vol. 48, no. 6, pp. 1839–1848, Jun. 2018.
[35] L. Long and J. Zhao, "Switched-observer-based adaptive neural control of MIMO switched nonlinear systems with unknown control gains," *IEEE Trans. Neural Netw. Learn. Syst.*, vol. 28, no. 7, pp. 1696–1709, Jul. 2017.
[36] W. He and Y. Dong, "Adaptive fuzzy neural network control for a constrained robot using impedance learning," *IEEE Trans. Neural Netw. Learn. Syst.*, vol. 29, no. 4, pp. 1174–1186, Apr. 2018.
[37] L. Long and J. Zhao, "Adaptive output-feedback neural control of switched uncertain nonlinear systems with average dwell time," *IEEE Trans. Neural Netw. Learn. Syst.*, vol. 26, no. 7, pp. 1350–1362, Jul. 2015.
[38] R. Skjetne, T. I. Fossen, and P. V. Kokotovic, "Adaptive maneuvering, with experiments, for a model ship in a marine control laboratory," *Automatica*, vol. 41, no. 2, pp. 289–298, 2005.
[39] R. Cui, L. Chen, C. Yang, and M. Chen, "Extended state observer-based integral sliding mode control for an underwater robot with unknown disturbances and uncertain nonlinearities," *IEEE Trans. Ind. Electron.*, vol. 64, no. 8, pp. 6785–6795, Aug. 2017.
[40] Y. Yuan, H. Yuan, Z. Wang, L. Guo, and H. Yang, "Optimal control for networked control systems with disturbances: A delta operator approach," *IET Control Theory Appl.*, vol. 11, no. 9, pp. 1325–1332, 2017.
[41] Y. Yuan, L. Guo, and Z. Wang, "Composite control of linear quadratic games in delta domain with disturbance observers," *J. Franklin Inst.*, vol. 354, no. 4, pp. 1673–1695, 2017.
[42] S.-L. Dai, C. Wang, and M. Wang, "Dynamic learning from adaptive neural network control of a class of nonaffine nonlinear systems," *IEEE Trans. Neural Netw. Learn. Syst.*, vol. 25, no. 1, pp. 111–123, Jan. 2014.
[43] W. He, H. Huang, and S. S. Ge, "Adaptive neural network control of a robotic manipulator with time-varying output constraints," *IEEE Trans. Cybern.*, vol. 47, no. 10, pp. 3136–3147, Oct. 2017.
[44] M. Chen and S. S. Ge, "Adaptive neural output feedback control of uncertain nonlinear systems with unknown hysteresis using disturbance observer," *IEEE Trans. Ind. Electron.*, vol. 62, no. 12, pp. 7706–7716, Dec. 2015.
[45] X. Jin, "Adaptive iterative learning control for high-order nonlinear multi-agent systems consensus tracking," *Syst. Control Lett.*, vol. 89, no. 3, pp. 16–23, 2016.

Shude He received the B.E. degree in automatic control from the Guangdong University of Technology, Guangzhou, China, in 2015. He is currently working toward the Ph.D. degree with the School of Automation Science and Engineering, South China University of Technology, Guangzhou, China.

His current research interests include adaptive and learning control systems and coordination and control of multiagent systems.

Min Wang (M'09) received the B.Sc. degree in mathematics and the M.Sc. degree in applied mathematics from the Bohai University, Jinzhou, China, in 2003 and 2006, respectively, and the Ph.D. degree in system theory from Qingdao University, Qingdao, China, in 2009.

She is a Visiting Scholar with the Department of Computer Science, Brunel University London, Uxbridge, United Kingdom. She is currently an Associate Professor with the School of Automation Science and Engineering, South China University of Technology, Guangzhou, China. She has authored or coauthored more than 50 papers published in international journals and conference proceedings. Her current research interests include intelligent control, dynamic learning, and robot control.

Dr. Wang was a recipient of the Excellent Doctoral Dissertations Award of Shandong Province in 2010, the Outstanding Graduate Award for Technological Innovation of Shandong Province in 2009, the Science and Technology New Star of Zhujiang, Guangzhou, in 2014, and the youth talent of Guangdong Tezhi Plan in 2016.

Shi-Lu Dai (S'09–M'11) received the B.Eng. degree in thermal engineering in 2002 and the M.Eng. and Ph.D. degrees in control science and engineering in 2006 and 2010, respectively, from Northeastern University, Shenyang, China.

He was a Visiting Student with the Department of Electrical and Computer Engineering, National University of Singapore, Singapore, from November 2007 to November 2009, and a Visiting Scholar with the Department of Electrical Engineering, University of Notre Dame, Notre Dame, IN, USA, from October 2015 to October 2016. Since 2010, he has been with the School of Automation Science and Engineering, South China University of Technology, Guangzhou, China, where he is currently a Professor. His current research interests include adaptive and learning control and distributed cooperative systems.

Fei Luo received the B.E. degree in computer science in 1982 and the M.E. and Ph.D. degrees in control science and engineering in 1986 and 1993, respectively.

From October 1990 to October 1992, he was a Visiting Scholar with the Kyushu Institute of Technology, Japan. He is currently a Professor with the School of Automation Science and Engineering, South China University of Technology, Guangzhou, China. He has authored or coauthored more than 80 papers in international journals and conferences. His research interests include intelligent control, motion control systems, and pattern recognition.